Dark Energy in M-Theory

Jonathan Tooker*
School of Physics and School of Materials Science and Engineering, Georgia Tech, Atlanta, GA, USA
(Dated: November 21, 2011)

Dark Energy is yet to be predicted by any model that stands out in its simplicity as an obvious choice for unified investigative effort. It is widely accepted that a new paradigm is needed to unify the standard cosmological model (SCM) and the minimal standard model (MSM). The purpose of this article is to construct a modified cosmological model (MCM) that predicts dark energy and contains this unity. Following the program of Penrose, geometry rather than differential equations will be the mathematical tool. Analytical methods from loop quantum cosmology (LQC) are examined in the context of the Poincaré conjecture. The longstanding problem of an external time with which to evolve quantum gravity is resolved. The supernovae and WMAP data are reexamined in this framework. No exotic particles or changes to General Relativity are introduced. The MCM predicts dark energy even in its Newtonian limit while preserving all observational results. In its General Relativistic limit, the MCM describes dark energy as an inverse radial spaghettification process. Observable predictions for the MCM are offered. AdS/CFT correspondence is discussed. The MCM is the 10 dimensional union of de Sitter and anti-de Sitter space and has M-theoretical application to the five string theories which lack a unifying conceptual component. This component unifies gravitation and electromagnetism.

arXiv:submit/0364607 [gr-qc] 21 Nov 2011

"The temporal order of events [*sic*] is irrelevant."

-Richard Feynman

I. INTRODUCTION

Observational evidence of dark energy emerged near the dawn of the millennium [1–3]. This data was only the latest in a growing list of disconcerting anomalies. Parity violation indicates that the geometric structure of reality is not well understood while the neutrino mass exposes the incompleteness of quantum theory. The spontaneous appearance of the universe from a big bang begs causality. If there is a cycle of universe birth and rebirth how is that reconciled with the Second Law of Thermodynamics? As the universe evolves forward from the big bang, the entropy increases steadily. The universe continues to strive toward thermodynamic equilibrium as gravity takes over and contraction begins. The end result should be the realization of maximum entropy but we see the microstate of our system is the same as when it started: one minimal structure. We are called into a Gibbsian paradox.

The gaps in our theory are most obvious when we look to the heavens and see them retreat from us under acceleration. Presumably all ordinary matter and energy connected by spacetime will attract but we observe repulsion. Numerous schemes have been devised in hopes of explaining the anomalous data to little avail. What is clear is this: dark energy can only be reconciled with our current theories if it was negligible in the past, then only over time did it grow to become the dominant energy in Nature [4].

In times of acknowledged crisis the scientific community turns toward philosophical analysis [5]. It is asked if synergy in new physics can be found; is there a simple unifying principle which remains undiscovered [6]? The MSM and the SCM cannot be reconciled without such a new discovery [7].

An early result in General Relativity was that a stationary universe would self-gravitate, clump and collapse to one singular point. Reasoning that Nature cannot be a temporary event, Einstein included the cosmological constant in his equations to provide the pressure needed to counterbalance this self-gravity. He sought to guarantee the perpetuity of Nature by the introduction of an arbitrarily tuned parameter; something no physicist can enjoy. Shortly after Λ was postulated, Hubble observed that the universe is not stationary [8]. Einstein was relieved to remove the constant with which only unstable solutions for a steady universe were generated.

Soon after and with much success, de Broglie postulated all moving objects have an associated wave [9]. Today, the wavefunction of the universe is considered throughout the literature. But what of the object, U, corresponding to this wave? What can be said about its evolution under the action of LQC? This article will discuss the properties of U in the framework of string theory.

A new paradigm is needed in physics and the MCM is such a construction. An excellent discussion of new physics is found in [7]. Section II of this paper will cover the mathematical foundations of the MCM. Beyond this, the physics of LQC are developed to introduce a novel new solution to dark energy. This naturally extends to non-perturbative string theory and grand unification.

* jonathan.t@gatech.edu

II. FOUNDATIONS

Perelman's proof of the Poincaré conjecture can be applied to LQC in a way not possible with other cosmologies. The conjecture is this: every simply-connected, closed three-manifold is homeomorphic to the three-sphere. Bojowald has shown that the divergent singularities of classical General Relativity do not exist in Nature [10]. Given this, the Poincaré conjecture can be applied to LQC as: every simply-connected, closed three-manifold is diffeomorphic to the three-sphere.

For convenience, this paper will manipulate the FLRW model. The size of the 3-space spanned by its x_i is characterized by a scale factor $a(t)$

$$\frac{\ddot{a}}{a} = -\frac{4\pi G}{3}\left(\rho + \frac{3p}{c^2}\right) + \frac{\Lambda c^2}{3} \tag{1}$$

Diagrams are used in physics to transmit information with a clarity not present in excessively quantified arguments. For example, the slope of the lightlike interval in the Minkowski diagram of special relativity (figure 1)is an excellent proxy for the scale factor a in the Minkowski metric. The MCM is a generalized geometric framework characterized by such physical proxy schema.

The Minkowski diagram is a convenient tool for qualitative analysis and will serve as the foundation on which the MCM is assembled. This diagram is a good approximant for arbitrary regions far from the origin. Near the origin, quantum contributions to (1) become dominant and the slope of the lightlike interval fails to characterize $a(t)$. This is will be discussed in section V. It has been shown that LQC adequately generates a period of inflation very near the origin which reduces to (1) at large volumes [11].

Nearly a century after Einstein we know that gravitational collapse will not snuff out the universe in the event of a big crunch. In the framework of quantum geometry, it has been demonstrated that Reimannian space is quantized [10]. Near the singularity, these discretized elements of volume exert a repulsive force which overcomes gravitational collapse and a classical singularity is forbidden [10]. The key result of this work is the deterministic evolution of solutions through the classical singularity [12–17]. In place of a big crunch, LQC predicts a series of temporally cyclic bounces where each bang is the result of a preceding crunch. This is illustrated in figure 2 which first appeared in [18].

The conformal equivalence of the Minkowski diagram and the Penrose diagram (figure 3) is trivial. The universe defined by I and II in the Penrose diagram travels forward through time and this motion constitutes a component of its 4-momentum. If momentum is conserved, the big bang must have thrown an equal amount of matter and energy along both time directions as in figure 4. This is not posed an assumption but rather an absolute fact of momentum-conserving Nature.

Regions III and IV of the Penrose picture are unphysical in the SCM. This fact stems from the big bang sin-

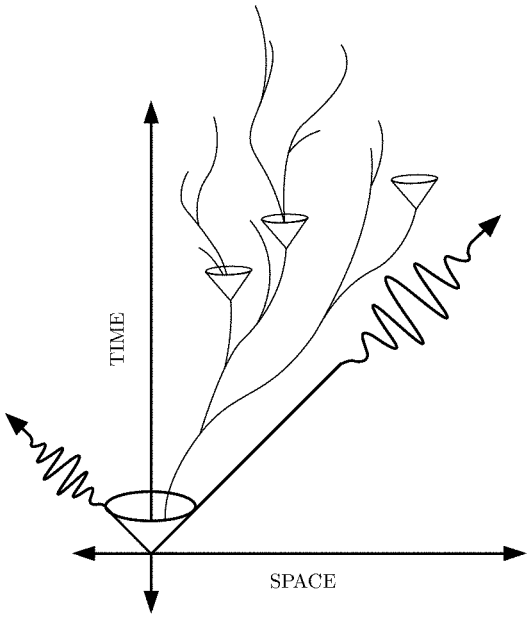

FIG. 1. The Minkowski lightcone of an event and myriad worldlines.

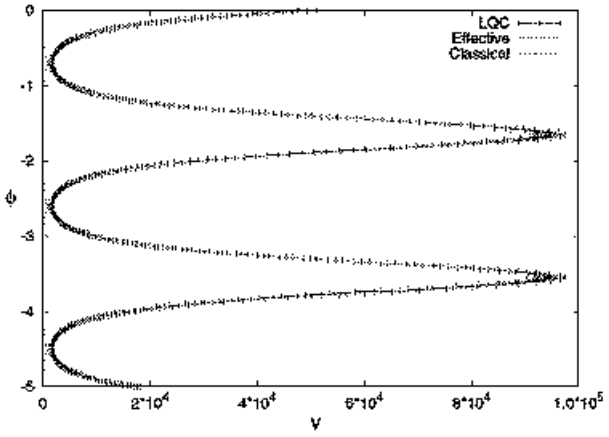

FIG. 2. [18] A modified Minkowski diagram: the vertical axis is what Ashtekar refers to as emergent time [19]. The nature of the motion is oscillatory as the Planck regime physics of quantum geometry cause bouncing. Rigorously, the vertical axis is the scalar field and horizontal is the expectation value of the volume operator operating on the wavefunction of the universe. This operator is a direct representation of the scale factor a.

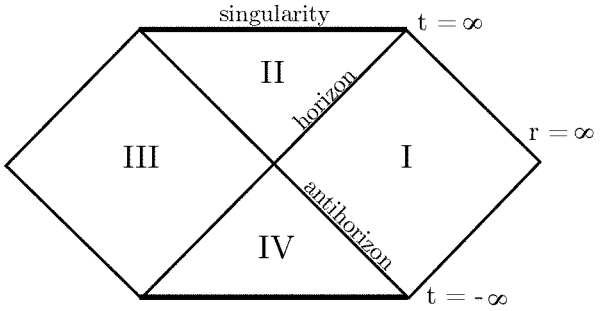

FIG. 3. Penrose diagram of conformal Schwarzchild geometry.

gularity forbidden in LQC. In the present divergence-free paradigm, all four regions are physical and coexist. Penrose's reverse time description of III and IV is accepted without question in the MCM; such a reverse time regime is needed to satisfy the momentum argument made above.

In figure 4, region A is a conformal map of Penrose regions I and II. Region B represents Penrose III and IV. Spacelike regions C and D are orthogonal to the Penrose diagram and do not appear in it.

A and B represent two universes propagating oppositely along the x_0 axis. One universe is the mirror image of the other so the bounce is topologically equivalent to the symmetric creation of a particle and an antiparticle which we will call U and $\bar{U}$. In the wave picture we view the bounce as a quantum decay to two time arrow eigenstates: $|t_+\rangle$ and $|t_-\rangle$.

$$\widehat{LQC}\,|bounce\rangle = |t_+\rangle + |t_-\rangle \tag{2}$$

$$\hat{T}\,|bounce\rangle = 0 \tag{3}$$

$$\hat{T}\,|t_\pm\rangle = \pm\,|t_\pm\rangle \tag{4}$$

$\hat{T}$ is the time arrow operator and $|t_i\rangle = U_i(x_0)$. U_i is the wavefunction of the 3-foliation on an observer at any proper time x_0. Following de Broglie, each U_i is both a particle and a cohesive wave packet propagating along the time axis. Together the axis and the wave form a 4D spacetime. The case of $k = 0$ is discussed in section III while $|t_\pm\rangle$ correspond to $k = \pm 1$.

$$ds^2 = dt_\pm^2 - a^2(t_\pm)\left(1 + \frac{kr^2}{4}\right)d\mathbf{r}^2 \tag{5}$$

The MCM states that the physics of grand unification is contained in the theory of pair creation in vacuum where the cosmological constant takes the form of a zero point energy [7, 20]. This duality is the unification of General Relativity and Maxwell's Equations.

$$T_{\mu\nu}^{vac} = \rho_{vac} g_{\mu\nu} \quad , \quad \Lambda = \frac{8\pi}{m_{Pl}^2}\rho_{vac} \tag{6}$$

III. SPACETIME

Before examining the root of dark energy let us clarify the physics of spacetime. Spacetime is a Hausdorff differentiable manifold. General Relativity dictates that matter and energy will gravitate if connected by spacetime.

$$G_{\mu\nu} + \Lambda g_{\mu\nu} = \frac{8\pi G}{c^4} T_{\mu\nu} \tag{7}$$

A recent development is this: information can be transmitted through the big bounces of LQC deterministically [16]. This new path of evolution opens avenues to new spacetime topologies [10]. With these physics in mind, let us fold space.

Given the periodicity in figure 2, the most natural thing is to impose a periodic boundary condition. Advanced metrical analysis of periodicity in spacetime dimensions is found in [21].

Consider the topological manipulations on spacetime illustrated in figure 5. To begin, wrap the time axis of figure 4 around a cylinder. U and $\bar{U}$ travel oppositely around the x_0 circle until the bounce occurs at $x_0 = \pm\pi$ in convenient polar units.

Observers occupy left and right movers on the x_0 circle. The big bang and crunch are identical and may be mapped into each other by twisting the x_0 circle into a figure eight. Twist it once further so that time reforms a circle with forward time in the clockwise direction for each universe. Finally, conserve 4-momentum at

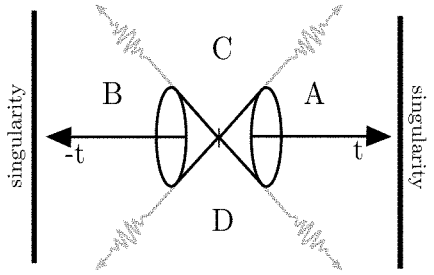

FIG. 4. Loop quantum cosmologies are finite in extent. Periodic boundary conditions are imposed the Minkowski diagram.

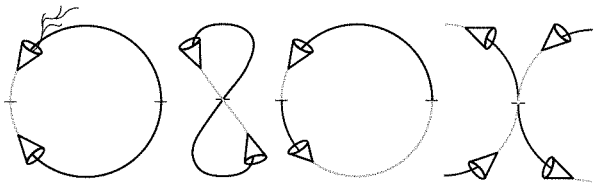

FIG. 5. The flat universes in 4 are mapped to spherical via wrapping. The lower universe, $\bar{U}$, is mapped to a hyperbolic universe via twisting. Grey intervals indicate the past as experienced by an observer in the adjacent cone. Horizontal hash marks indicate LQC bounces.

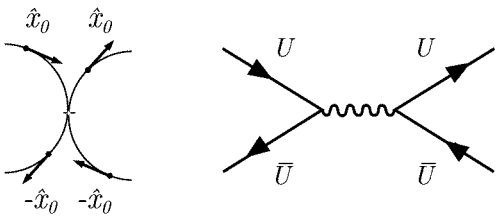

FIG. 6. A duality transformation between the geometric and particle pictures.

the bounce so it is schematically clear.

To alleviate problems with human intuition in perceiving the flow of time let us do the following. Replace figure 5(d) with the familiar Feynman diagram where a rigorous framework is well established for dealing with interacting parties moving in different directions through time. Figure 6 illustrates the equivalence of the geometric and particle views.

The WMAP data rules out the curvature of the universe postulated here [22]. To avoid this contradiction let us assume WMAP observes a superposition of $|t_+\rangle$ and $|t_-\rangle$ so that $|t_\star\rangle = \alpha\ |t_+\rangle + \beta\ |t_-\rangle$ as in figure 7. Then the WMAP samples two oppositely curved spaces which obey the superposition principle. The result is the observation of flat space. The metric along $|t_\star\rangle$ is given by $k = 0$ in (5).

$$ds^2 = dt_\star^2 - a^2(t_\star)d\mathbf{r}^2 \tag{8}$$

Schrödinger's cat experiment explains that in the absence of an observation wavefunctions are diffuse. When the box is closed the cat is both dead and alive. Likewise, observers will never be able to say if they belong to $|t_+\rangle$ or $|t_-\rangle$. The wavefunction is diffuse and the postulation of $|t_\star\rangle$ is confirmed. When an observation cannot be made, both possibilities must coexist as a superposition of states.

In quantum mechanics the arrow of time is not specified; Feynman diagrams are useful because time flows generally to the right in the "timeless" interactions they describe. The duality in the Minkowski picture and the Feynman picture is completed in figure 8.

IV. DARK ENERGY

Dark energy arises naturally from the interaction of U and $\bar{U}$. Unwrap figure 5(a) as in figure 9(a) so that U and $\bar{U}$ converge forward in time toward the big crunch along a 1D manifold. The nature of the evolution on this manifold is the crux of the present argument. In figure 9(b) two massive particles m_1 and m_2 gravitate along the x_i axis and we must be true to ourselves when we declare time to be naught more than a fourth orthogonal dimension in spacetime. If m_1 and m_2 gravitate, shall we not conclude that U and $\bar{U}$ gravitate identically? Gravitation is a global property of all matter and energy connected by spacetime.

The gray interval at each end of figure 9(a) represents the past as experienced by an observer in the adjacent cone. This interval is defined as all points on an observer's worldline where $z > 0$. There exists a bijection between redshift and time; spacetime is divided into subsets as in figure 10.

$$z + 1 = a(t_0)/a(t') \tag{9}$$

$$z \in [z_{min}, z_{max}] \quad \rightarrow \quad x_0 \in [0, \pi] \tag{10}$$

$$Past \in [0, x_0^0)\ ,\ Future \in (x_0^0, \pi] \tag{11}$$

$$Present \in [x_0] \tag{12}$$

Supernovae observed to accelerate away from observers on Earth reside exclusively in the past. We cannot observe astrophysical objects as they are today; that light has yet to reach our instruments. In 3-space, objects such as type Ia supernovae may have x_i greater or smaller than the x_i of an observer. However, in the inertial frame defined by said observer, the high-z condition of the supernovae data can be expressed as $x_0^0 \gg x_0'$ where x_0' is the proper time of the observable. Observers will always be

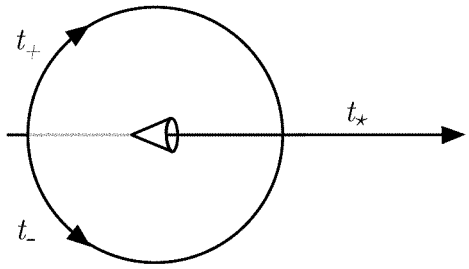

FIG. 7. Observable space is postulated to be a linear superposition of the wavefunctions of the foliations on $t_\pm$. In the paradigm of quantum field theory, the sudden appearance of U and $\bar{U}$ is described according to virtual pair creation.

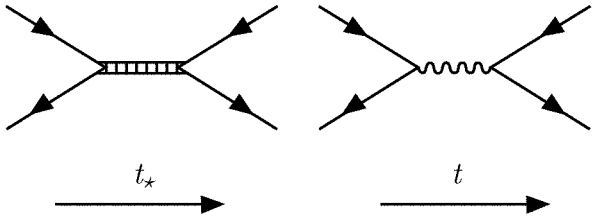

FIG. 8. In the Feynman diagrams of QED and QCD time generally flows to the right and anti-particles are denoted with arrows pointing in reverse time. The relevant construction for LQC, a graviton exchange, is shown for clarity.

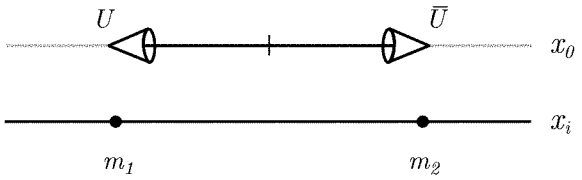

FIG. 9. If m_1 and m_2 are defined to lie on the x_i axis they will undergo attraction. Similarly U and $\bar{U}$ should undergo gravitational attraction according to the metric defined on the manifold that connects them. The vertical hash marks the bounce.

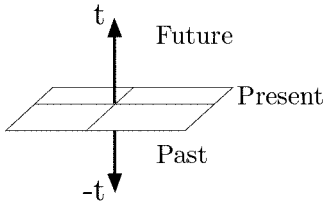

FIG. 10. The geometric structure of psychological time.

deeper into $\bar{U}$'s gravitational well than the astrophysical objects they observe.

The state $|t_\star\rangle$ may be decomposed into two states with opposite curvature; however, $|t_\pm\rangle$ experience symmetric convergence to the bounce. When observers operate on $|t_\star\rangle$ to detect dark energy there is no cancellation as with their respective curvatures. As U and $\bar{U}$ near the bounce, the gradient in curvature will increase at $z = 0$ with respect to fixed comoving high-z observables.

This is an alternative interpretation of data suggesting that the more distant an object lies, the more quickly it accelerates away from us. Acceleration is relative and in the paradigm presented here it is more intuitive to claim that we are accelerating away from the past, toward the future. This is an inverse radial spaghettification process where acceleration of images away from us indicates the event horizon of the bounce accelerating toward us.

Dark energy has been explained in the framework of Einstein's equations with time varying cosmological constant. Specifically, Λ evolves monotonically with increasing t_+ and t_- but is cyclic in $t_\star$. In the early universe this effect is negligible when U and $\bar{U}$ are far apart. As the universe ages, dark energy increases. In classical cosmology it is taken for granted that the big crunch is out there somewhere in spacetime. In the MCM that idea takes one step forward: as matter falls into the big crunch its event horizon will expand outward in time.

V. GEOMETRY

Following the bounce a period of inflation is geometrically represented by the lightcone opening wider than $\pi/2$ radians near the origin. When inflation concludes, the directional anisotropy of the lightcone (a 4D hypercone) is hidden from observers who only access 4π steradians of isotropic solid angle. This evolution is described in figure 11. An isotropic 3-space grows inside the light cone which inflates through 4π srad before closing on itself. This closure leaves a preferred direction in the cosmos such as the one seen in the multipole analysis of the WMAP data.

Every 4D hypercone (Minkowski lightcone) generates a dual cone, i.e.: the existence of one hypercone implies the existence of another as in figure 4. This geometry supplements the momentum argument for the physicality of $\bar{U}$ in the Penrose diagram made in section II. If we consider the 4D geometry of inflation described by a cone and its dual cone as in figure 12, we recover the geometric structure of psychological time.

MCM solutions will evolve through the classical singularity. Consequently, the union of Penrose II and IV must be conformally equivalent to I and III. When this is true the antihorizon and the horizon cannot be distinguished as in figure 13. No distinction can be made between the universe and the parallel universe. If U and $\bar{U}$ are separate and coexist as required by the Law of Conservation

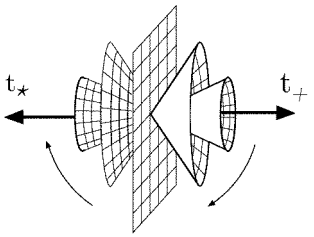

FIG. 11. The closure of the foliation on $t_\pm$ defines $\pm t_\star$. The good axis defined by the WMAP multipole analysis constitutes observational evidence for $|t_\star\rangle$. $t_\star$ and t_+ appear parallel in this projection but $\hat{t}_\star \cdot \hat{t_\pm} = 0$ according to (13).

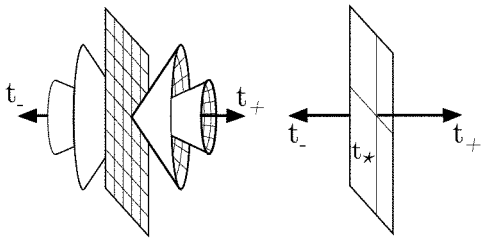

FIG. 12. In the larger view, the closure of the foliation is a plane. In one picture the cone encompasses 4π srad and in the other it encompasses 2π srad. This is an artifact of the spin geometry of the graviton propagator that connects U and $\bar{U}$

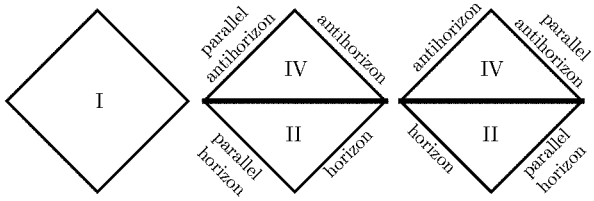

FIG. 13. The horizon is merely an optical effect. At the antihorizon we label this effect dark energy and call it inverse radial spaghettification. Inflation is the time reverse process on the horizon. The age of the universe cannot be gauged due to this optical distortion. The entropy of a black hole is proportional to its area because they always appear circular when viewed from the origin; there can be no texture to distinguish it from a non-horizon sphere. The remaining two dimensions of the MCM reside on the on the black hole and the temporal sphere. This opens new avenues to EPR physics.

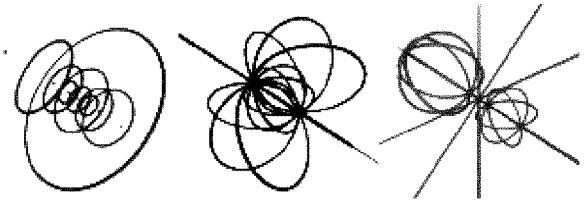

FIG. 14. Stereographic projection of the 3-sphere outlines the geometry of the fabric of time. Intersection of these lines and circles defines an orthogonal triad [23].

of Momentum, then an additional degree of freedom must be introduced. This is a third component of time beyond "up" and "down." We have labeled these three components $\{t_+, t_-, t_\star\}$. This system is most easily visualized in figure 7. At the bounce these three dimensions satisfy the cross product. The relation of $\{ijk\}$ and $\{+-\star\}$ in $\mathbf{a}\times\mathbf{b} = \epsilon_{ijk}\hat{e}_i a_j b_k$ is defined by the stereographic projection of the 3-sphere decomposed in figure 14.

$$\hat{t}_+ \times \hat{t}_- = \hat{t}_\star \tag{13}$$

Three classes of curvature solve (1) and each represents an orthogonal dimension on the 3-sphere: flat parallels, spherical hypermeridians and hyperbolic meridians. In lieu of a single 4D spacetime, time and space are partially decoupled with a specific 3-space embedded in each time dimension.

We give further credence to the MCM by noting that the present cosmos is not invariant under parity conjugation. Note that for observers in $|t_+\rangle$ left is "out" and right is "in". When figure 7 undergoes parity conjugation around $t_\star$ the diagrammatic structure of the universe is unchanged but $t_\pm \to t_\mp$. The physics of this asymmetry is that the spherical space defined on the hypermedian becomes a hyperbolic space on the meridian.

The small deviations from flatness in allowable spherical and hyperbolic cosmologies are mirrored in the small cross sections for parity violating processes. It is possible that parity violation can be used to measure curvature in the 3-sphere.

Observers have access to one dimension of time: $t_\star$. Together with the three spatial dimensions of the foliation we assemble the four dimensions of everyday physics.

It must be noted that the meridians and hypermeridians also foliate universes and these wavefunctions are not confined to the axes. They travel on the 3-sphere but extend into the 3-ball such that their tails overlap the $k = 0$ wavefunction at rest on the observer. As such, in the very high energy regime, observers in $t_\star$ may access the 3 spatial dimensions embedded in t_+ and t_- giving them access to 10 total dimensions as predicted by string theory.

Observers are confined to lines and the metric along each time axis has been defined. Special Relativity defines the time axis as the world line of the observer. On the other hand, observables occupy the space between the lines where a more complex metric is defined according to Ricci flow [24]. It is the high-z condition on the supernovae data that puts these objects far enough away that Ricci flow contributions to the metric become non-negligible. The microwave background is then due to the onset of hyperturbulence rather than baryogenesis.

The wildest assumption ever made in physics is that the universe appears isotropic at every point within it. This is based on nothing. If the distance to a surface (the CMB) is the same in every direction, then the surface is a sphere and the observer must be at its center. In the SCM, the universe is x years old. This is extrapolated from the distance measured to the CMB. If observers on Earth look at the same point in the sky for 12 hours they see a point in the CMB $2x$ light years away from the initial observation and they are in thermal equilibrium. The speed of light is an upper bound on the transmission of information; therefore, the big bang interpretation of the CMB is unphysical. In the paradigm of the MCM, the universe always appears isotropic because MCM observers are confined to the origin just as observers in special relativity are confined to the ct axis.

The derivations of dark energy and a preferred axis in the cosmos speak for themselves. Beyond that, the existence of $t_\star$ can be derived via the Penrose diagram of LQC without reference to the philosophically charged Schrödinger experiment. The WMAP observes flat space because it only measures the comoving components of $t_\star$. U and $\bar{U}$ are multiply derived as well. String theory predicts a 10 dimensional high energy regime and this is present in the MCM. Parity is violated in Nature and parity is not conserved in the MCM. A geometrically robust cosmological model has been presented.

VI. AdS_5/CFT_4 CORRESPONDENCE

Figure 7 is a 12 dimensional system consisting of three 3-balls embedded on the surface of another 3-ball. Observers in this system are prohibited from accessing x_0^+ and x_0^- without going through a black hole and the resulting system is 10D. These 10 dimensions can be decomposed into a 5D de Sitter space and a 5D anti-de Sitter space. Each space is an ordinary 4D spacetime coupled to a fifth dimension that describes the curvature.

In string theory the only dimensionful parameter is the length of the string l_s. Figure 7 is composed of three strings and two vertices. Spherical $|t_+\rangle$ and hyperbolic $|t_-\rangle$ both have $l_s = \pi$ while flat $|t_\star\rangle$ has $l_s = 2$. Each of these states is a 4D spacetime and does not compose a five dimensional space. The fifth dimension of dS_5 and AdS_5 space is defined by the ratio $l_\pm/l_\star$. Using this, string theory can be reformulated as an M-theory with no reference to dimensionful parameters.

When a string is assigned to each line in 14, we derive a candidate for the full non-perturbative structure of string theory. The orthogonal triad at each vertex is composed of one parallel, one meridian and one hyper-

meridian suggesting that the full extent of this structure is entirely contained in figure 7.

At first glance, figure 7 cannot encompass the entire theory because the geometry does not reflect parity violation. This can be resolved by rescaling the lengths of the strings. The Poincaré conjecture only states diffeomorphism with the 3-sphere; there is no reason to assume $l_\pm = \pi$. Nature seems to suggest an obvious choice of ratio.

$$l_+ = \frac{1+\sqrt{5}}{2} \tag{14}$$

$$l_\star = 1 \tag{15}$$

$$l_- = \frac{1-\sqrt{5}}{2} \tag{16}$$

Gravity in the 3-ball is equal to a local field theory on the 3-sphere. From figure 12 it is geometrically obvious that $t_\star$ is the boundary where the supersymmetric $N = 4$ Yang-Mills theory is defined. We have also seen that $t_\star$ is the present as it serves as the boundary between t_+ and t_-. By (11) the present corresponds to a single point on which a time arrow cannot be defined. This is why (2) is not written $\widehat{LQC}\,|bounce\rangle = |t_+\rangle + |t_-\rangle + |t_\star\rangle$.

$$\hat{T}\,|t_\star\rangle = 0 \tag{17}$$

$$|t_\star\rangle = |bounce\rangle \tag{18}$$

VII. DISCUSSION

We have assigned a spatial 3-sphere $\{x_1, x_2, x_3\}$ to each dimension of the temporal sphere $\{x_0^+, x_0^-, x_0^\star\}$. Space serves as the radial coordinate of the temporal ball just as time serves as the radial coordinate in the 3+1 dimensional space of General Relativity. The distinction of temporal and spatial spheres is mirrored in the spacelike and timelike regions of the Minkowski diagram.

By alternating temporal and spatial spheres, diameters are mapped to circumferences and it is clear that the MCM is a fractal matrix theory of infinite complexity. This embedding and reembedding is the physical manifestation of T-duality. As such, the frequency of oscillation in figure 2 is on the order of the Planck time in a larger universe. The MCM is the full realization of the Holographic Principle which states that the entirety of the universe is contained in every piece of it. This is shown in figure 15.

A long standing problem in quantum field theory is that the energy density of the vacuum is infinite. In the paradigm presented here, $t_\star$ has no "volume" in the temporal 3-sphere. Thus, a finite energy density is obtained when infinitely large energy is divided by infinitely small "volume."

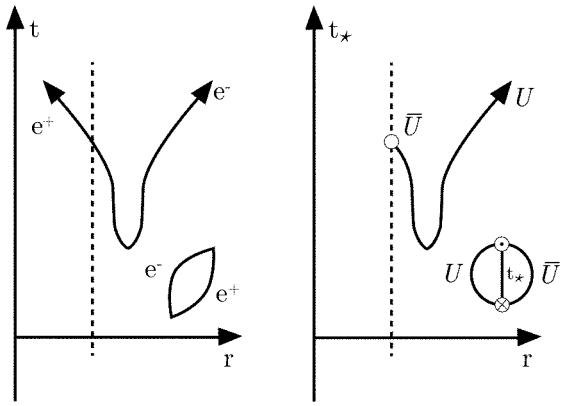

FIG. 15. The Feynman diagrams of gauge theory generate surfaces which represent interacting strings [25]. On the left: electromagnetic pair creation near the horizon. On the right: polarized gravitational pair creation.

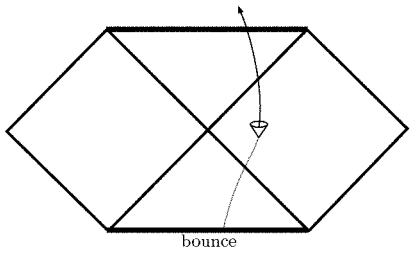

FIG. 16. Penrose diagram of the MCM. The worldline goes outside of the box.

The MCM explains why time does not appear in quantum mechanics. Quantum mechanics is a theory of Hilbert spaces but in the MCM we see there is no need for functions defined on time to go to zero at infinity. We have come full circle and confirmed Einstein's intuition that Nature is not a temporary event but rather an eternal one. There are no endings, only new beginnings.

The MCM contains 12 local dimensions: 9 of space and 3 of time. Observers are forbidden from accessing two time dimensions and the result is a 10 dimensional system of worldsheets defined on the 3-sphere. Its parallels, meridians and hypermeridians form a network of closed and open strings.

In classical physics orthogonality is defined by rotations of $\pi/2$ radians. The MCM forges a tangency between gravity and electromagnetism along the vacuum polarization vector near the horizon. We have introduced an new component of orthogonality defined by $\phi/3$ complex hyperadians. The irrational ratio ϕ/π is the source of difficulty in computing non-perturbative quantum gravity with differential equations. Conformal mapping preserves boundary conditions of differential equations in both the past and the future.

The MCM exploits the mathematical strength of geometry to carefully define a set of conformal mappings that only preserve boundary conditions in the present where CFT_4 is defined. Due to ϕ/π, additional boundary condi-

tions cannot be accommodated. Irrationality in the ratio of string lengths is the root of turbulence. Feynman's comment on temporal order is reflected in the MCM; the past and the future are irrelevant. There is only now.

When in the course of the universe the antihorizon becomes imminent, MCM specific specific observables will arise. Parity violation is due to the off-axis Ricci flow contributions in the metric. Near the bounce foliated wavefunctions on $t_{\pm}$ will contribute strongly to the superposition on the observer. As a result, cross sections for parity violating processes should change near the bounce.

It is unlikely that the time dependence of Λ can be measured directly given the very long times involved. However, in the region very near the bounce the rapidly increasing gradient would be observable as a lowering of the high-z requirement for dark energy. Interestingly, the historical record of the Mayan civilization indicates that just such a cosmogenesis event will occur on December 21, 2012 [26]. This strange coincidence makes the present an optimal time for new observations.

ACKNOWLEDGEMENTS

Thank you Manny Gonzales, Emily Marie Hancock and Jean Bellissard for invaluable discussions. Thank you to Naresh Thadhani and Ignacio Taboada for funding while this research was conducted. To Georgia Tech for funding this research with the Presidential Fellowship. Thank you to my mother, Helene Gutfreund, for everything else.

[1] B. P. Schmidt, ASTROPHYSICAL JOURNAL **507** (1998).
[2] Reiss et al., The Astronomical Journal **116**, 1009 (1998).
[3] Permutter et al., The Astrophysical Journal **517**, 565 (1999).
[4] Bahcall et al., Science **284**, 1481 (1999).
[5] T. Kuhn, *The Structure of Scientific Revolutions* (Univeristy of Chicago Press, 1962).
[6] D. Bigatti and L. Susskind, *M-Theory and Quantum Geometry* (Kluwer Academic publishers., 2000), chap. The Holographic Principle, pp. 179–225.
[7] A. D. Dolgov, Physics of Atomic Nuclei **71**, 651 (2008).
[8] E. Hubble, Astrophysical Journal **64**, 321 (1926).
[9] L. de Broglie, Ph.D. thesis, Sorbonne (1924).
[10] M. Bojowald, Physical Review Letters **86**, 5227 (2001).
[11] M. Bojowald, Physical Review Letters **89**, 261301 (2002).
[12] M. Bojowald, Class Quant Grav **17**, 1489 (2000).
[13] M. Bojowald, Class Quant Grav **17**, 1509 (2000).
[14] M. Bojowald, Class Quant Grav **18**, 1055 (2001).
[15] M. Bojowald, Class Quant Grav **18**, 1071 (2001).
[16] Ashtekar et al., Physical Review Letters **96**, 141301 (2006).
[17] A. Ashtekar and P. Singh, Class Quant Grav **28** (2011).
[18] Ashtekar et al., Physical Review D **75**, 024035 (2007).
[19] A. Ashtekar, in *Invisible Universe: Proceedings of the Conference* (2010).
[20] Y. B. Zeldovich, Soviet Physics Uspekhi **11** (1968).
[21] C. Misner, Physical Review Letters **22**, 1071 (1969).
[22] Spergel et al., Astrophysical Journal Supplement Series **170**, 377 (2007).
[23] C. Rocchini, http://en.wikipedia.org/wiki/3-sphere.
[24] S. Brendle, *Ricci Flow and the Sphere Theorem* (American Mathematical Society, 2010).
[25] J. de Boer, introduction to AdS/CFT correspondence.
[26] J. M. Jenkins, *Maya Cosmogenesis 2012: The True Meaning of the Maya Calendar End-Date* (Bear & Company, 1998).